Transactions of the International Wire & Cable Symposium

Temperature Response of OPGW with Mixed Armored Aluminum Covered Steel Wires and Aluminum Alloy Wires Submitted to Short-Circuit

Sergio Colle, Marcelo A. Andrade, João T. Pinho, João C. V. da Silva, Mauro Bedia, Carlos E. Veiga, and Júlio N. Scussel

DOI:10.3841/TIWCS.2008.20

Volume 1

2008

Selected papers from the 55th IWCS held November 2006

ISSN 1941-4242

Temperature Response of OPGW with Mixed Armored Aluminum Covered Steel Wires and Aluminum Alloy Wires Submitted to Short-Circuit

Sergio Colle[1], Marcelo A. Andrade[2], João T. Pinho[3], João C. V. da Silva[2], Mauro Bedia[2], Carlos E. Veiga[1], and Júlio N. Scussel[1]

[1]Department of Mechanical Engineering / Federal University of Santa Catarina
Florianópolis, Santa Catarina, Brazil
+55-48-32342161 / 32340408 · colle@emc.ufsc.br
[2]Prysmian Telecomunicações Cabos e Sistemas do Brasil S.A.
Sorocaba – São Paulo – Brazil
+55-15-32359209 · marcelo.andrade@prysmian.com
[3]Department of Electric Engineering / Federal University of Pará
Belém – Pará – Brazil
+55-91-32111299 · jtpinho@ufpa.br

Abstract

The present paper focuses on the heat transfer problem that describes the heat conduction effects in an OPGW submitted to short-circuit. An analytical solution is proposed which accounts for the effect of the temperature gradients in the aluminum covered steel wires, and the contact thermal resistance in the effective contact surface between the fiber extruded aluminum tube and the aluminum covered steel wires. The numerical results are compared with results previously obtained and reported in the 54th IWCS Conference, for an OPGW with armored steel wires with the same dimensions. The analytical solution is expressed in terms of integral equations, which can be numerically solved in terms of the heat flux, as well as the temperature of the tube and the wires. The present approach is appropriate and effective to make design parameter sensibility analysis as well as for parameter estimation of the thermal contact resistance. The numerical results reported here show that the aluminum layer of the steel wires are very effective in reducing the electrical resistance of the cable and therefore, the temperature gradients in the steel wire as well as the temperature increase in the aluminum tube.

Keywords: OPGW, Short-circuit; unsteady heat-transfer.

1. Introduction

A novel design of OPGW manufactured with aluminum covered steel wires and aluminum alloy is reported in [1]. The authors pointed out the advantage of mixing aluminum covered steel wires and aluminum alloy wires to increase the current carrying capacity. The current carrying capacity of an OPGW depends mainly on the electric resistance of its conductor components, as is the case of the extruded aluminum tube and the armored wires. As is shown in [2, 3], the maximum temperature achieved in the extruded aluminum tube depends not only on the electric resistance of the conductors, but also on the thermal contact resistance between the armored wires and the tube, and the thermal conductivity of the material of the armored wires. The mechanical design of an OPGW should take in to account the maximum temperature achieved in the tube in order to prevent annealing. During the short-circuit it may happens that the differential strain of OPGW components may brake the aluminum tube or may lead to mechanical damage of the armored wires (bird-caging). An optimized OPGW should be designed in such a way that for a given short-circuit current, a minimized temperature rise should be achieved at the end time of the short-circuit, in order to reduce differential thermal strain. The electric current of the OPGW focused here is assumed to be distributed in parallel association through the tube, the aluminum cover of the wires, and the steel wires themselves. Therefore, thermal effects caused by temperature gradients as well as by the covering layer thickness should be taken into account, in order to investigate the effect of the electric current on the temperature variation of each conductor with time. As made in [3], in order to simplify the present analysis, it is further assumed here that the electric resistance of the wire is evaluated as a function of the average wire temperature over its cross section.

2. Basic Equations

In the present analysis the skin effects due to the intensive short-circuit current are neglected. The skin effect for an OPGW as focused here, according to [4], may result in a temperature gradient around 10°C over the cross section of the extruded aluminum tube. This temperature gradient is around 4% of the maximum temperature expected in the aluminum tube. It is assumed here that the heat loss at the outer surfaces of the armored wires to the surrounding medium is neglected. The optic fibers gel inside the extruded aluminum tube is assumed to have very low thermally conductivity, so that the inner surface of the extruded tube can be consider to be insulated. The temperature gradient over the cross section of the tube is also neglected.

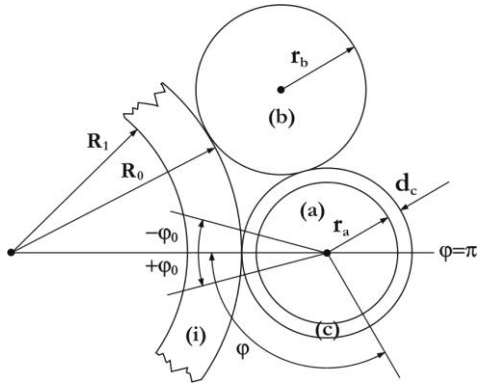

Figure 1. Cross section geometry of the OPGW

The mathematical approach given in [3] is used here for analyzing the conjugate heat conduction problem. Both the aluminum covered wire (a) and the uncovered wire (b) are supposed to be in thermal contact with the tube, but in no thermal contact with each other. The effective thermal contact angle for both wires (a) and (b) is assumed equal to φ_o as shown in Figure 1.

2.1 Aluminum Tube

The energy balance for the tube (i), by assuming no thermal gradient over the cross section of the tube is shown to be governed by the following dimensionless equation [5, 6, 7]:

$$\frac{d\theta_i}{d\tau} = p_i\left(\theta_i,\bar{\theta}_a,\bar{\theta}_b,\bar{\theta}_c\right) - \frac{2}{\pi}\alpha_c\beta_c F_{oc}\phi_{oc}(\tau) - \frac{2}{\pi}\beta_b F_{ob}\phi_{ob}(\tau) \quad (1)$$

where $\theta = \frac{T - T_o}{T_o}$, $\tau = t/\Delta t_{sc}$, T_o is the initial temperature, Δt_{sc} is the short-circuit duration time, $\bar{\theta}_a$, $\bar{\theta}_b$, and $\bar{\theta}_c$ are the average temperatures over the cross section of wire core (a) and wire (b), and the aluminum covering layer (c), respectively. $F_{ob} = k_b \Delta t_{sc} / \rho_b c_b r_b^2$ is the Fourier number respective to wire (b), $F_{oc} = k_c \Delta t_{sc} / \rho_c c_c ((r_c + r_a)/2)^2$ is the Fourier number respective to the aluminum cover layer (c) of wire core (a), $\alpha_c = 2d_c/(r_a + r_c)$, d_c is the thickness of the covering layer (c), $\beta_b = N_b\sqrt{1+\kappa_b^2}\,\rho_b c_b \pi r_b^2 / \rho_i c_i \pi(R_o^2 - R_1^2)$, $\kappa_b = 2\pi(R_o + r_b)/L$ is the pitch ratio of wire (b),

$\beta_c = N_a\sqrt{1+\kappa_c^2}\,\rho_c c_c \pi\left(\frac{r_a + r_c}{2}\right)^2 / \rho_i c_i \pi(R_o^2 - R_1^2)$, $\kappa_c = \kappa_a$, $\kappa_a = 2\pi(R_o + r_a + d_c)/L$ is the pitch ratio of wire (a), $\phi_{oa} = \int_0^{\varphi_o} \phi_a(\varphi,\tau)d\varphi$, $\phi_a = q_a'' r_a / k_a T_o$, $\phi_{ob} = \int_0^{\varphi_o} \phi_b(\varphi,\tau)d\varphi$, $\phi_b = q_b'' r_b / k_b T_o$, $\phi_c = q_c'' r_c (r_a + r_c)/2 d_c k_c T_o$, and q'' represents the heat flux density in the surface (W/m^2). The dimensionless heat flux is expressed in terms of the derivative of the dimensionless temperature by $\phi_a(\varphi,\tau) = \frac{\partial\theta_a}{\partial\eta}(1,\varphi,\tau)$, where $\eta = r/r_a$ and $\phi_b(\varphi,\tau) = \frac{\partial\theta_b}{\partial\eta}(1,\varphi,\tau)$, where $\eta = r/r_b$.

The Joule heating source term of equation (1) can be obtained by assuming parallel association of tube (i), wires (a) and (b), and the aluminum cover (c). Since the Joule effect is assumed to be uniformly distributed over the volume of the conductors, it can be assumed that the electric resistance of each conductor is evaluated at its average temperature over the cross section according to the equation $R = R_{20} f(\bar{\theta})$, where f is the temperature depended electric resistivity function. This assumption is justified by experimental results [3]. In terms of the physical variables, the dimensionless equation for p_i can be written as follows [6],

$$p_i = q_i f_i(\theta_i) f_a(\bar{\theta}_a)^2 f_b(\bar{\theta}_b)^2 f_c(\bar{\theta}_c)^2 / q^2 \quad (2)$$

where

$$q = \lambda_a\lambda_b\lambda_c f_a f_b f_c + f_i(N_a\lambda_b\lambda_c f_b f_c + N_a\lambda_a\lambda_b f_a f_b + N_b\lambda_a\lambda_c f_a f_c) \quad (3)$$

$q_i = (I^2 \Delta t_{sc}) R_{20i}\lambda_a^2\lambda_b^2\lambda_c^2 / \rho_i c_i \pi(R_o^2 - R_1^2) L T_o$,

$\lambda_a = R_{20a}/R_{20i} = \rho_{20a}\pi(R_o^2 - R_1^2)\sqrt{1+\kappa_a^2} / \rho_{20i}\pi r_a^2$,

$\lambda_b = R_{20b}/R_{20i} = \rho_{20b}\pi(R_o^2 - R_1^2)\sqrt{1+\kappa_b^2} / \rho_{20i}\pi r_b^2$,

$\lambda_c = R_{20c}/R_{20i} = \rho_{20c}\pi(R_o^2 - R_1^2)\sqrt{1+\kappa_c^2} / \rho_{20i}\pi(r_c^2 - r_a^2)$, L is the length of tube (i) corresponding to one turn of the wires around the tube N_a, N_b, and $N_c = N_a$ are the numbers of wires (a) and (b) and cover layer (c), respectively, ρ represents the specific mass, c represents the specific heat, R_{20} represents the electrical resistance at 20°C, ρ_{20} represents the electrical resistivity at 20°C, and k represents the thermal conductivity.

2.2 Covered wire (a)

The energy balance in wire (a) is governed by a differential equation which can be written in dimensionless form as follows [3, 6],

$$\frac{1}{\eta}\frac{\partial}{\partial\eta}\left(\eta\frac{\partial\theta_a}{\partial\eta}\right) + \frac{p_a}{F_{oa}} = \frac{1}{F_{oa}}\frac{\partial\theta_a}{\partial\tau} \quad (4)$$

where $\eta = r/r_a$, $F_{oa} = k_a \Delta t_{sc} / \rho_a c_a r_a^2$ is the Fourier number respective to wire core (a),

$p_a = q_a f_i(\theta_i)^2 f_a(\bar{\theta}_a) f_b(\bar{\theta}_b)^2 f_c(\bar{\theta}_c)^2 / q^2$,

$q_a = (I^2 \Delta t_{sc}) R_{20i}\lambda_a\lambda_b^2\lambda_c^2 / \rho_a c_a \pi r_a^2 L_a T_o$, and

$L_a = L\sqrt{1+\kappa_a^2}$ is the length of the effective thermal contact surface strip of width $e_a = 2 r_a \varphi_o$.

The initial conditions for θ_i and θ_a are given by,

$$\theta_i(0) = \theta_a(\eta,\varphi,0) = 0 \quad (5)$$

From the overall energy balance in wire (a) it can be shown that the average temperature over the cross section of the wire can be expressed as

$$\frac{d\bar{\theta}_a}{d\tau} = p_a\left(\theta_i,\bar{\theta}_a,\bar{\theta}_b,\bar{\theta}_c\right) + \frac{2F_{oa}}{\pi}\phi_{oa}(\tau) \quad (6)$$

From equation (5) it follows that the initial condition for equation (6) is $\bar{\theta}_a(0) = 0$.

2.3 Uncovered wire (b)

Similarly to equation (4), for wire (b) the following equation holds,

$$\frac{1}{\eta}\frac{\partial}{\partial\eta}\left(\eta\frac{\partial\theta_b}{\partial\eta}\right) + \frac{p_b}{F_{ob}} = \frac{1}{F_{ob}}\frac{\partial\theta_b}{\partial\tau} \quad (7)$$

where $\eta = r/r_b$,

$p_b = q_b f_i(\theta_i)^2 f_a(\bar{\theta}_a)^2 f_b(\bar{\theta}_b) f_c(\bar{\theta}_c)^2 / q^2$,

$q_b = (I^2 \Delta t_{sc}) R_{20i} \lambda_a^2 \lambda_b \lambda_c^2 / \rho_b c_b \pi r_b^2 L_b T_o$, and $L_b = L\sqrt{1+\kappa_b^2}$ is the length of the effective thermal contact surface strip of width $e_b = 2 r_b \varphi_o$.

The initial condition for θ_b is given by,

$$\theta_b(\eta, \varphi, 0) = 0 \tag{8}$$

From the overall energy balance for wire (b) it can be shown that the average temperature over the cross section of the wire can be expressed as

$$\frac{d\bar{\theta}_b}{d\tau} = p_b\left(\theta_i, \bar{\theta}_a, \bar{\theta}_b, \bar{\theta}_c\right) + \frac{2F_{ob}}{\pi}\phi_{ob}(\tau) \tag{9}$$

From equation (8) it follows that the initial condition for equation (9) is $\bar{\theta}_b(0) = 0$.

The heat flux at the thermal contact interface between the wire (b) and the tube (i) is related to a Biot number by the following equation [3, 6],

$$\phi_b(\varphi, \tau) = -B_{ib}\left(\theta_b(1, \varphi, \tau) - \theta_i(\tau)\right) \tag{10}$$

for $0 \le \varphi \le \varphi_o$, where $B_{ib} = h_b r_b / k_b$ is the Biot number, h_b is the heat transfer coefficient related to the effective heat transfer contact area between the wire and the tube. The heat flux is assumed to vanish for $\varphi_o < \varphi \le \pi$.

2.4 Covering layer (c)

Since the material of the layer (c) has high thermal conductivity it can be assumed that there is no thermal resistance in the radial direction. Therefore the diffusion equation reduces to a one-dimensional equations in terms of the circumferential variable $\bar{s} = (r_c + r_a)\varphi / 2$. The details of the derivation of the mentioned equation, accounting for the heat flux respective to wire (a), and the heat flux at the interface of thermal contact between the layer (c) and the tube (i) is reported in [6]. The following equation is obtained

$$\frac{\partial^2 \theta_c}{\partial \varphi^2} + \frac{p_c}{F_{oc}} + (\phi_c - \gamma \phi_a) = \frac{1}{F_{oc}} \frac{\partial \theta_c}{\partial \tau} \tag{11}$$

where $\gamma = k_a(r_a + r_c) / 2k_c d_c$,
$p_c = q_c f_i(\theta_i)^2 f_a(\bar{\theta}_a)^2 f_b(\bar{\theta}_b)^2 f_c(\bar{\theta}_c) / q^2$,
$q_c = (I^2 \Delta t_c) R_{20i} \lambda_a^2 \lambda_b^2 \lambda_c / \rho_c c_c \pi (r_c^2 - r_a^2) L_c T_o$, and L_c, which is equal to L_a, is the length of the effective thermal contact surface strip of width $e_c = 2 r_c \varphi_o$.

The initial condition associated to equation (11) is given by

$$\theta_c(\varphi, 0) = 0 \tag{12}$$

Because of the symmetry of temperature distribution over layer (c) respective to angle φ it follows,

$$\frac{\partial \theta_c(0, \tau)}{\partial \varphi} = \frac{\partial \theta_c(\pi, \tau)}{\partial \varphi} = 0 \tag{13}$$

By assuming perfect thermal contact between the wire core (a) and the covering layer (c), no temperature discontinuity exists at the contact interface. Therefore

$$\theta_a(1, \varphi, \tau) = \theta_c(\varphi, \tau) \tag{14}$$

for $0 \le \varphi \le \pi$.

The heat flux at the interface of thermal contact between layer (c) and tube (i) is related to the Biot number by the following equation [6],

$$\phi_c(\varphi, \tau) = -B_{ic}\left(\theta_c(1, \varphi, \tau) - \theta_i(\tau)\right) \tag{15}$$

for $0 \le \varphi \le \varphi_o$, where $B_{ic} = h_c r_c (r_a + r_c) / 2 d_c k_c$ is the Biot number, h_c is the heat transfer coefficient related to the effective heat transfer contact area between the wire and the tube. The heat flux is assumed to vanish for $\varphi_o < \varphi \le \pi$.

The overall energy balance in layer (c), leads to the following differential equation [6],

$$\frac{d\bar{\theta}_c}{d\tau} = p_c\left(\theta_i, \bar{\theta}_a, \bar{\theta}_b, \bar{\theta}_c\right) + \frac{F_{oc}}{\pi}(\phi_{oc}(\tau) - \gamma \phi_{oa}(\tau)) \tag{16}$$

The initial condition for the above equation, according to equation (12) is given by $\bar{\theta}_c(0) = 0$.

The solution of equation (4) with the initial condition given by equation (5) is obtained by the method of Green's functions for the Neumann problem, as presented in Appendix A. The mathematical background can be found in [8]. The temperature distribution at the outer surface of the wire, $\theta_a(1, \varphi, \tau)$, according to equation (A6) of Appendix A can be written as follows,

$$\begin{aligned} \theta_a(1, \varphi, \tau) &= \int_0^\tau p_a(\theta_i, \bar{\theta}_a, \bar{\theta}_b, \bar{\theta}_c) d\tau' \\ &+ \frac{2F_{oa}}{\pi} \int_0^\tau \left[g_{oa}(\tau, \tau') \phi_{oa}(\tau') d\tau' + \right. \\ &\left. \sum_{n=1}^{\infty} g_{na}(\tau, \tau') \phi_{na}(\tau') \cos n\varphi \right] d\tau' \end{aligned} \tag{17}$$

where $\phi_{na}(\tau) = \int_0^\pi \phi_a(\varphi, \tau) \cos n\varphi \, d\varphi$; $n = 0, 1, 2....$

$$g_{oa}(\tau, \tau') = 1 + \sum_{m=1}^{\infty} e^{-\beta_m^{o^2} F_{oa}(\tau - \tau')} \tag{18}$$

$$g_{na}(\tau, \tau') = 2 \sum_{m=1}^{\infty} \frac{e^{-\beta_m^{n^2} F_{oa}(\tau - \tau')}}{(1 - n^2 / \beta_m^{n^2})} \tag{19}$$

where β_m^n is the root of the derivative of the Bessel function of first kind of integer order $J_n'(\beta_m^n)$; $n = 0, 1, 2....$

Similarly, the solution of equation (7) with the initial condition given by equation (8) for the boundary condition of prescribed heat flux ϕ_b is given by,

$$\theta_b(1,\varphi,\tau) = \int_0^\tau p_b(\theta_i,\bar{\theta}_a,\bar{\theta}_b,\bar{\theta}_c)d\tau' + \frac{2F_{ob}}{\pi}\int_0^\tau \left[g_{ob}(\tau,\tau')\phi_{ob}(\tau')d\tau' + \sum_{n=1}^{\infty} g_{nb}(\tau,\tau')\phi_{nb}(\tau')cosn\varphi \right] d\tau' \quad (20)$$

where $\phi_{nb}(\tau) = \int_0^{\varphi_o} \phi_b(\varphi,\tau)cosn\varphi\, d\varphi$; $n = 0, 1, 2...$

$$g_{ob}(\tau,\tau') = 1 + \sum_{m=1}^{\infty} e^{-\beta_m^{o2} F_{ob}(\tau-\tau')} \quad (21)$$

$$g_{nb}(\tau,\tau') = 2\sum_{m=1}^{\infty} \frac{e^{-\beta_m^{n2} F_{ob}(\tau-\tau')}}{(1-n^2/\beta_m^{n2})} \quad (22)$$

In a similar way, the solution of equation (11) satisfying the initial condition given by (12) can be expressed as follows,

$$\theta_c(\varphi,\tau) = \int_0^\tau p_c(\theta_i,\bar{\theta}_a,\bar{\theta}_b,\bar{\theta}_c)d\tau' + \frac{F_{oc}}{\pi}\int_0^\tau \left[(\phi_{oc}(\tau') - \gamma\phi_{oa}(\tau')) + 2\sum_{n=1}^{\infty} e^{-n^2 F_{oc}(\tau-\tau')}(\phi_{nc}(\tau') - \gamma\phi_{na}(\tau'))cosn\varphi \right] d\tau' \quad (23)$$

where $\phi_{nc}(\tau) = \int_0^{\varphi_o} \phi_c(\varphi,\tau)cosn\varphi\, d\varphi$; $n = 0, 1, 2...$

The boundary condition given by equation (14) can be imposed by the Galerkin condition as follows,

$$\int_0^\pi [\theta_a(1,\varphi,\tau) - \theta_c(\varphi,\tau)]cosp\varphi d\varphi = 0 \quad ; p = 0,1,2,... \quad (24)$$

Similarly, the boundary conditions given by (10) and (15) can be respectively imposed by the Galerkin conditions as follows,

$$\int_0^{\varphi_o} [\phi_b + B_{ib}(\theta_b(1,\varphi,\tau) - \theta_i(\tau))]\, cosp\varphi = 0 \quad (25)$$

$$\int_0^{\varphi_o} [\phi_c + B_{ic}(\theta_c(\varphi,\tau) - \theta_i(\tau))]cosp\varphi = 0 \quad (26)$$

; $p = 0,1,2,....$

The ordinary differential equations (1), (6), (9), and (16) and the boundary conditions given by (24), (25), and (26) can be solved in terms of the unknown functions $\theta_i, \bar{\theta}_a, \bar{\theta}_b, \bar{\theta}_c, \phi_{na}, \phi_{nb}$, and ϕ_{nc}, for $n = 1,2,....,N$, where N is arbitrarily chosen in order to reach a given accuracy. A numerical solution can be obtained by reducing the boundary conditions to integral equations, with the help of the series expansions given by equations (17), (20), and (23).

The integral equations and the respective system of algebraic equations, expressed in terms of the unknown heat flux coefficients and the unknown temperatures $\theta_i, \bar{\theta}_a, \bar{\theta}_b$, and $\bar{\theta}_c$ are presented in Appendix B.

3. Discussion of Results

3.1 Predicted results

Two types of cable are analyzed. The first one is the cable OPGW 13,4 06 FO manufactured by Prysmian, which consists of ten armored zinc coated steel wires. The second cable is the OPGW 12,4 48 FO manufactured by Prysmian, which consists of mixed armored aluminum covered steel wires and aluminum alloy wires. In order to present and analyze the predicted results, the OPGW 13,4 06 FO will be taken as reference. The predicted results respective to the case of five mixed aluminum covered steel wires and five aluminum alloy wires are compared with the predicted results corresponding to the case of ten steel wires. It is assumed that the wires as well as the tube have the same geometrical configuration and size as for OPGW 13,4 06 FO. The electrical and the thermophysical proprieties of the materials of the cables were supplied by Prysmian.

The parameters Λ_b and Λ_c are defined in Appendix B, where Λ_c can be expressed as $\Lambda_c = 2B_o F_{oc}\varphi_o/\pi$, where $B_o = 2h_c\varphi_o\Delta t_c/\rho_a c_a\pi(r_a + d_c)$. The parameter Λ_b can be expressed in terms of Λ_c as $\Lambda_b = \Lambda_c\rho_c c_c\pi d_c(r_a + r_c)/2\rho_a c_a\pi r_a^2$.

Figure 2 illustrates the effect of the contact angle φ_o on the maximum temperature achieved in the tube, as a function of the dimensionless thermal contact resistance parameter B_o. The thermal contact resistance parameter B_o is chosen to be 0.3, which is the numerical value experimentally determined from short-circuit tests of OPGW 13,4 06 FO, as reported in [3].

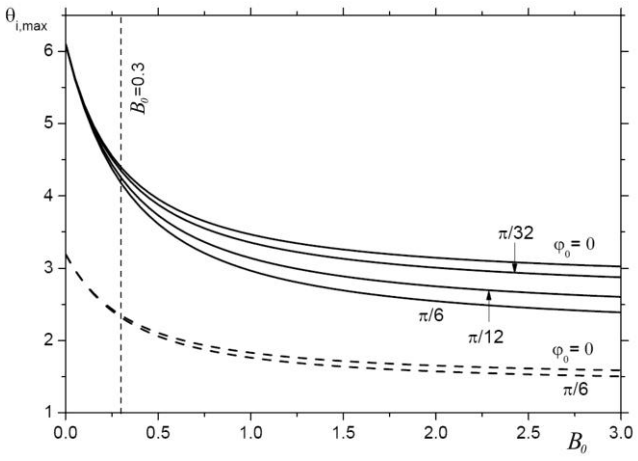

Figure 2. Maximum temperature achieved in the tube for the case of ten aluminum covered steel wires, for various values of the contact angle φ_o, $d_c/r_c = 0$ (——), and $d_c/r_c = 0.1$ (- - -)

For the sake of comparison of the predicted results, B_o is assumed to be constant for both, the heating and the cooling time periods of the short-circuit test. As will be seen later, this parameter varies with time during the cooling period.

Figure 2 shows that the maximum temperature achieved in the tube is sensible with B_o for values around 0.3, for all aluminum cover layer thickness ratio d_c / r_c up to 0.1. Figure 2 also shows that the limiting-curve corresponding to vanishing contact angle is pretty close to curves corresponding to the small contact angle size of the cable tested and reported in [3], which is around $\pi / 35$. Since the limiting-case corresponding to vanishing contact angle can be chosen to represent the real cases, only the especial cases corresponding to vanishing contact angle are presented in the next figures.

Figure 3 illustrates the effect of the aluminum cover layer thickness on the maximum temperature achieved in the tube, as a function of B_o.

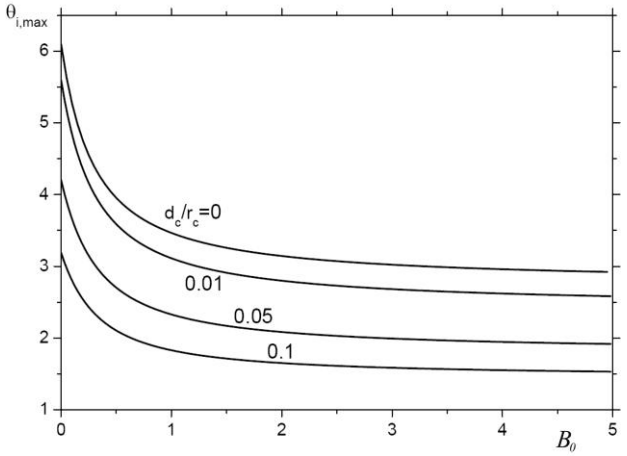

Figure 3. Maximum temperature achieved in the tube for the case of ten aluminum covered steel wires, for various values of d_c / r_c

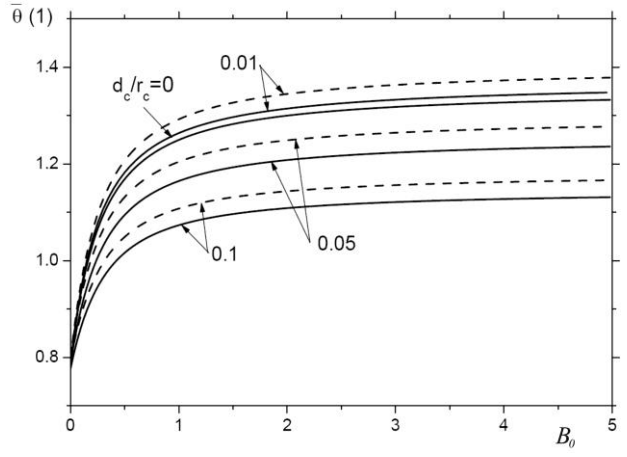

Figure 4. Temperature rise of the aluminum cover layer (c) (- - -) and the steel core (a) (——) at the end time of the short-circuit, for the case of ten aluminum covered steel wires

The effect of the aluminum layer is to reduce the maximum temperature achieved in the tube, for any value of the thermal contact resistance number. This also holds for the experimentally determined value of B_o equal to 0.3, for all cover layer thickness tested. The effect of the layer thickness is to increase the wire temperature at the end of the heating process, as illustrated in Figure 4. This effect compensates the decrease of the maximum temperature achieved in the tube.

Figure 5 shows the effect already observed in the preceding figures, for the temperature variation with time, for the tube, wire steel core, and the aluminum cover layer. The average cross section temperature of the steel core (a) and the aluminum cover layer (c) are shown to be pretty close, for all time considered.

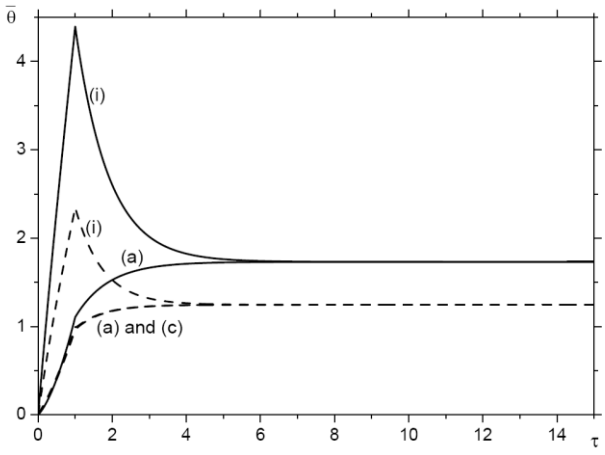

Figure 5. Temperature variation with dimensionless time $\tau = t / \Delta t_c$; $\Delta t_c = 0.5s$, for the case of ten aluminum covered steel wires (a), for $d_c / r_c = 0$ (——), $d_c / r_c = 0.1$ (- - -), and $B_o = 0.3$

Figure 6 illustrates the case of five aluminum covered steel wires alternated with five aluminum alloy wires. The overall effect of the aluminum cover layer (c) on the maximum temperature achieved in the tube is similar to that shown in Figure 3.

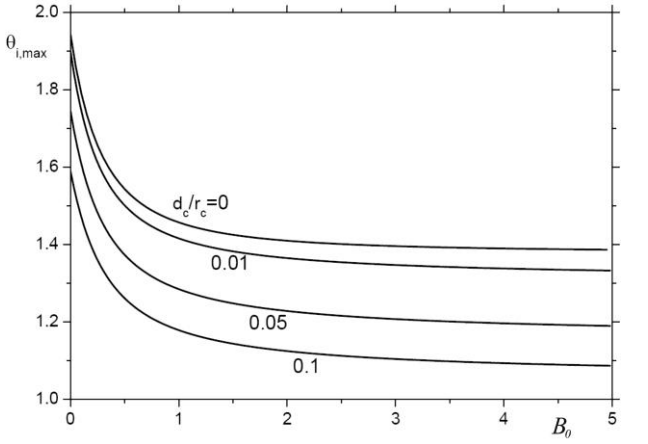

Figure 6. Maximum temperature achieved in the tube for the case of five aluminum covered steel wires and five aluminum alloy wires, for various ratios of d_c / r_c

However as Figure 6 shows, the maximum temperature reduction due to the aluminum cover layer is more effective in comparison to the case illustrated in Figure 3.

Figure 7 shows that the temperature achieved in the aluminum alloy wires at the end time of the short-circuit test, is pretty close to the temperature achieved in the tube. This is also shown in Figure 8, which illustrates how effective are the aluminum alloy wires in reducing the maximum temperature achieved in the tube.

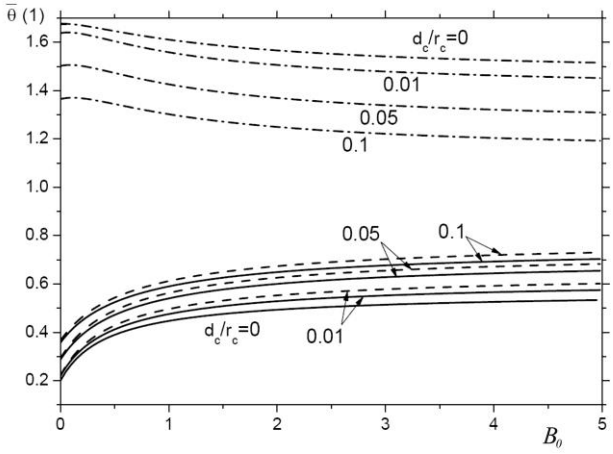

Figure 7. Temperature rise of the wires at the end time of the short-circuit for the case of five aluminum covered steel wires and five aluminum alloy wires (– – –) aluminum cover (c); (——) steel core (a); (–·–·–) aluminum alloy (b)

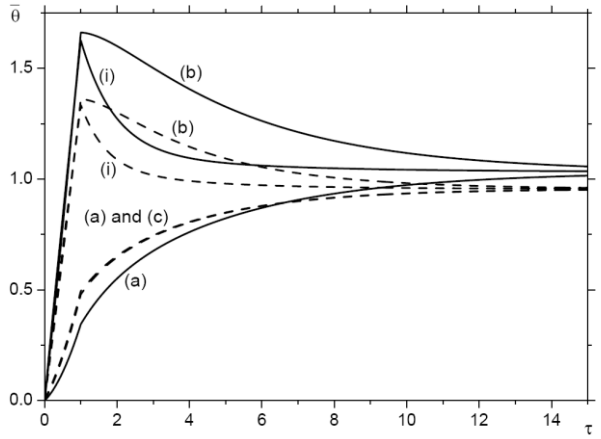

Figure 8. Temperature variation with dimensionless time for the case of five aluminum covered steel wires (a) and five aluminum alloy wires (b), for $d_c / r_c = 0$ (——), $d_c / r_c = 0.1$ (– – –), and $B_o = 0.3$

Figure 9 shows the comparison of predicted results of the maximum temperature achieved in the tube for both cases analyzed. The maximum temperature reduction for the case of five aluminum alloy wires is greater than the maximum temperature reduction for the case of ten aluminum covered steel wires.

It should be remarked that the maximum temperature achieved in the tube is less sensitive in respect to parameter B_o in the second case.

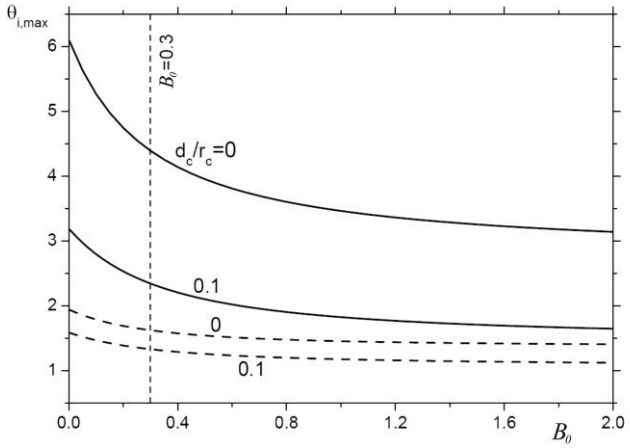

Figure 9. Comparison of the maximum temperature achieved in the tube for the case of ten aluminum covered steel wires (——) and the case of five aluminum covered steel wires and five aluminum alloy wires (– – –)

3.2 Comparison with experimental results

The description of the short-circuit test as well as the fault current test of OPGW can be found in [9]. The comparison of the predicted results with the experimental results obtained from short-circuit tests of OPGW 13,4 06 FO is shown in Figure 10. The results obtained from a simplified model that accounts only for the effects of the thermal capacitance of the tube and the wires (TCM model as described in [5]) are also plotted. It is shown from this figure that the simplified model underestimates the maximum temperature achieved in the tube. The simplified model also underestimates the temperature of the tube during the cooling time period. For the present model B_o is fitted against the experimental values of the tube temperature.

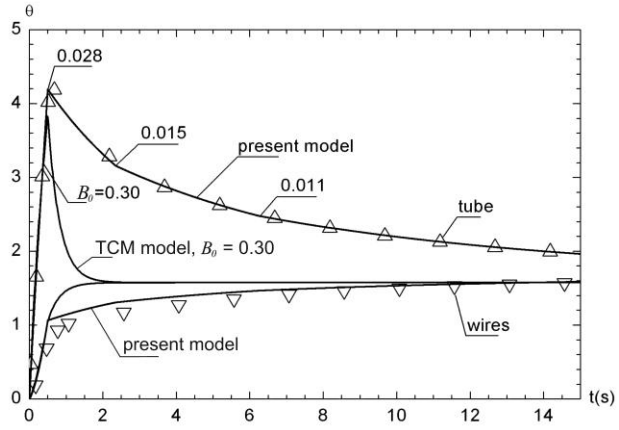

Figure 10. Predicted temperature distributions in the tube and the wire fitted piecewise with parameter B_o, compared with the experimental results of the temperature in the outer surface of the tube, for $\Delta t_c = 0.5s$ and $I = 7.7kA$

While in the heating time period the wires show to be in good mechanical and thermal contact with the aluminum tube, it is not the

case in the cooling time period. During this time, the cable oscillation due two its fast thermal expansion, may reduce the pressure of the wires on the aluminum tube, and therefore reduces the effective thermal contact.

Figure 11 shows the predicted results plotted against the experimental results obtained form short-circuit tests of cable OPGW 12,4 48 FO. The cable has four aluminum alloy wires (AAW) of diameter equal to 2.67 mm and seven aluminum covered steel wires (ACSW) of the same diameter. The outer diameter of the aluminum tube is 7.1mm.

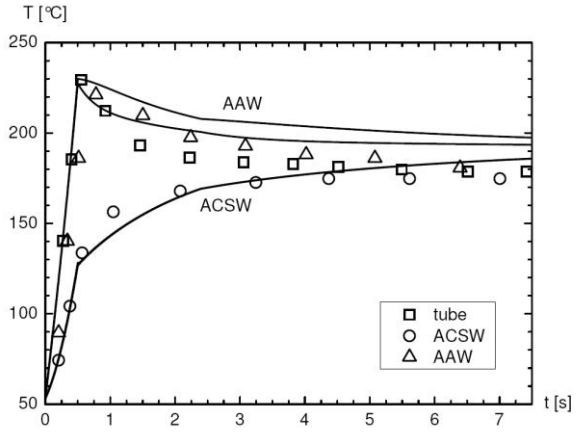

Figure 11. Predicted temperature distributions in the tube and the wires, fitted piecewise with parameter B_o, compared with the experimental results of the temperature in the outer surface of the tube, for $\Delta t_c = 0.5s$ and $I = 9.8kA$

The parameter B_o is fitted against the experimental values of the tube temperature. It is found that the best fitted value of B_o for the heating time period is 0.4, for which $h\varphi_o = 7.475kW/m^2 K$. For the cooling time period $B_o = 0.2$ for $t < 2.4s$ and $B_o = 0.1$ for $t > 2.4s$. Its worth to mention that for the heating time period, the numerical value obtained for B_o is close to its numerical value experimentally determined for the case of cable OPGW 13,4 06 FO. Figure 11 shows that the present model overestimates the steady-state limit temperature by 15°C. The temperature deviation may be explained by the fact that there is a cooling effect of the wires, due to the cable oscillation during the cooling time period. It should be remained that for the adiabatic condition as assumed in the present theory, the predicted steady-state limit-temperature depends only on the total energy stored in the cable. On the other hand, the cooling of the cable due to its oscillation induced by the short-circuit current, depends strongly on the wires thermal conductivity. The cooling effect is expected to be much more intense for OPGW 12,4 48 FO, because of the higher thermal conductivity of both, the aluminum alloy wires and the aluminum cover layer, in comparison to the thermal conductivity of the zinc coated steel wires of cable 13,4 06 FO.

4. Conclusions

The heat transfer effects due two the heating caused by short-circuit of an OPGW composed of armored aluminum covered steel wires and aluminum alloy wires is analyzed. The thermal effect caused by the aluminum covering layer as well as the aluminum alloy on the maximum temperature achieved in the extruded tube is investigated. It is shown that the thermal contact resistance in the interface of effective thermal contact between the tube and the wires may play an important role in the design of this type of conductor. It is shown also that the aluminum alloy wires are much more effective in reducing the maximum temperature achieved in the aluminum tube than the aluminum cover layer of the steel wires. The analytical solution reported here is highly sensitive with the physical and the geometrical parameters of the electric conductors. Sensibility to design parameters is an important feature for thermo-mechanical design of OPGW, as well as for experimental characterization and validation of design parameters.

5. References

[1] L-R. Sales Casals, F. Sangalli, F. Della Corte, J. Martin, and A. Ginocchio, "Fibers into Aliminum Extruded Tube (FiALT), A New Tecnology that Matches with Utilities Distribution Networks Needs", *Proceeding of the 54rd IWCS / Focus Conference, Providence, Rhode Island, USA* , (2005).

[2] S. Colle and M. de A. Andrade, "On the thermal contact resistance effects in aluminum-galvanized steel wires OPGW submitted to a short-circuit test" *Proceeding of the 53rd IWCS / Focus Conference, Philadelphia, Pa., USA* , (2004).

[3] S. Colle, M. de A. Andrade, M. Bedia, J. T. Pinho, K. L. Z. Glitz, C. E. Veiga, and J. N. Scussel, "Limit-Solutions for the Heat Transfer in OPGW Submitted to Short-circuit Test", *Proceeding of the 54rd IWCS / Focus Conference, Providence, Rhode Island, USA* , (2005).

[4] M. Zunec, F. Jakl and I. Ticar, "Skin effect impact on current density distribution in OPGW cables" *Electrotechnical Review*, 70 (1-2): 17-21, (2003).

[5] S. Colle, "Technical Reports No. 1-5 to Pirelli Telecommunication Cables and Systems of Brazil," *Department of Mechanical Engineering / UFSC*, (2003-2004).

[6] S. Colle, "Analytical Solutions for the Heat Conduction in Armored OPGW Submitted to Short-Circuit" (in Portuguese), Report No. 6 - Prysmian Telecomunicações Cabos e Sistemas do Brasil S/A, *Department of Mechanical Engineering / UFSC*, (2006).

[7] S. Colle, M. de A. Andrade, J. T. Pinho, J. C. V da Silva, M. Bedia, C. E. Veiga, and J. N. Scussel, "Temperature Response of OPGW with Armored Aluminum Covered Steel Wires Submitted to Short-Circuit", *Proceeding of the 55rd IWCS / Focus Conference, Providence, Rhode Island, USA*, (2006).

[8] I. Stakgold, "Boundary Value Problems of Mathematical Physics – Vol. II," *Macmillan*, (1968)

[9] R. S. Madge, S. Barret and H. Grad, "Performance of Optical Wires During Fault Current Tests", *IEE Transactions on Power Delivery*, 4 (3), (July, 1989).

Appendix A - Solution by the Green's Function Method

The Green's function for the Neumann problem associated to equation (4) and initial condition by (5) of the text, according to the dimensionless variables taken here, is the solution of the following partial differential equation [8],

$$-\frac{1}{\eta}\frac{\partial}{\partial\eta}\left(\eta\frac{\partial g}{\partial\eta}\right)+\frac{1}{F_{oa}}\frac{\partial g}{\partial\tau} = \frac{\delta(\eta-\eta')\delta(\varphi-\varphi')\delta(\tau-\tau')}{\eta F_{oa}}-\frac{2}{\pi} \tag{A1}$$

satisfying the following boundary conditions,

$$\frac{\partial g}{\partial\varphi}=0 \text{ for } \varphi=0 \text{ and } 0\le\eta\le 1 \tag{A2}$$

$$\left.\frac{\partial g}{\partial\varphi}\right|_{\varphi=0}=\left.\frac{\partial g}{\partial\varphi}\right|_{\varphi=\pi} \tag{A3}$$

and the initial condition given by

$$g(\eta,\varphi,\tau;\eta',\varphi',\tau)=0 \tag{A4}$$

where $\int_0^\tau\int_0^\pi\int_0^1\delta(\eta-\eta')\delta(\varphi-\varphi')\delta(\tau-\tau')d\eta'd\varphi'd\tau'=1.$

The Green´s function physically means a 2D temperature distribution over a semi-circle region, caused by a concentrated infinite heat source located at the point located at the coordinates η' and φ', applied at time τ', under the condition of vanishing heat flux at the boundary of the region.

The solution of equation (A1) satisfying the boundary conditions (A2) and (A3) and the initial condition given by equation (A4) is the following [6].

$$g(\eta,\varphi,\tau;\eta',\varphi',\tau')=\frac{2}{\pi}+\frac{2}{\pi}\sum_{m=1}^{\infty}e^{-\beta_m^{o\,2}F_{oa}(\tau-\tau')} \times\frac{J_o(\beta_m^o\eta)J_o(\beta_m^o\eta')}{J_o{}^2(\beta_m^0)}+\frac{4}{\pi}\sum_{m,n=1}^{\infty}e^{-\beta_m^{n\,2}F_{oa}(\tau-\tau')} \times\cos(n\varphi)\cos(n\varphi')\frac{J_n(\beta_m^n\eta)J_n(\beta_m^n\eta')}{(1-n^2/\beta_m^{n\,2})J_n{}^2(\beta_m^n)} \tag{A5}$$

where J_n; $n=0,1,2,...$ is the Bessel function of the first kind of integer order and β_m^n are the eigen-values, which are the roots of $J_n'(\beta_m^n)=0$; $n=0,1,2,...$.

The solution of equation (4) with the initial condition given by equation (5), for the boundary condition of prescribed heat flux $\phi_a(\varphi,\tau)$ at the interval $[0,\alpha]$ and vanishing heat flux at the interval $[\alpha,\pi]$ is the following,

$$\theta_a(\eta,\varphi,\tau)= \int_0^1\int_0^\pi\int_0^\tau g(\eta,\varphi,\tau;\eta',\varphi',\tau')p_a(\theta_i,\bar\theta_a,\bar\theta_b,\bar\theta_c)\eta'd\eta'd\varphi'd\tau' + F_{oa}\int_0^\tau\int_0^\alpha g(\eta,\varphi,\tau;1,\varphi',\tau')\phi_a(\varphi',\tau')d\varphi'd\tau' \tag{A6}$$

By replacing g from equation (A5) in (A6) the following equation is obtained

$$\theta_a(\eta,\varphi,\tau)=\int_0^\tau p_a(\theta_i,\bar\theta_a,\bar\theta_b,\bar\theta_c)d\tau' + F_{oa}\int_0^\tau\int_0^\alpha\left[\frac{2}{\pi}+\frac{2}{\pi}\sum_{m=1}^{\infty}e^{-\beta_m^{0\,2}F_{oa}(\tau-\tau')}\frac{J_o(\beta_m^o\eta)}{J_o(\beta_m^o)} +\frac{4}{\pi}\sum_{m,n=1}^{\infty}\frac{e^{-\beta_m^{n\,2}F_{oa}(\tau-\tau')}J_n(\beta_m^n\eta)}{(1-n^2/\beta_m^{n\,2})J_n(\beta_m^n)} \times\cos(n\varphi)\cos(n\varphi')\right]\times\phi_a(\varphi',\tau')d\tau' \tag{A7}$$

Appendix B - Integral Equations and Numerical Solution

By replacing θ_a given by equation (17) and θ_c given by equation (23) in equation (24) and by performing the integrals in the angle φ, it leads to the following integral equation

$$\int_0^\tau\left(F_{oc}\gamma+2F_{oa}\,g_{oa}(\tau,\tau')\right)\phi_{oa}(\tau')d\tau' - F_{oc}\int_0^\tau\phi_{oc}(\tau')d\tau' = \pi\left[\int_0^\tau p_c(\theta_i,\bar\theta_a,\bar\theta_b,\bar\theta_c)d\tau'-\int_0^\tau p_a(\theta_i,\bar\theta_a,\bar\theta_b,\bar\theta_c)d\tau'\right] \tag{B1}$$

for $p=0$ and

$$\int_0^\tau\left[F_{ob}\gamma\,e^{-p^2F_{ob}(\tau-\tau')}+F_{oa}g_p(\tau,\tau')\right]\phi_{pa}(\tau')d\tau' - F_{ob}\int_0^\tau e^{-p^2F_{ob}(\tau-\tau')}\phi_{pb}(\tau')d\tau'=0 \tag{B2}$$

for $p=1,2,...,N$.

By replacing θ_b given by equation (20) in equation (25), and by performing the integrals in the angle φ it leads to

$$\frac{\phi_{ob}(\tau)}{\Lambda_b}+\int_0^\tau\left[g_{ob}\phi_{ob}+\sum_{n=1}^{\infty}g_{nb}\frac{sen\,n\varphi_o}{n\varphi_o}\phi_{nb}\right]d\tau' = \frac{\pi}{2F_{oa}}\left[\theta_i(\tau)-\int_0^\tau p_b(\theta_i,\bar\theta_a,\bar\theta_b,\bar\theta_c)\,d\tau'\right] \tag{B3}$$

for $p=0$ and

$$\frac{\phi_{pb}(\tau)}{\Lambda_b}+\int_0^\tau\left[g_{ob}+\frac{sen\,p\varphi_o}{p\varphi_o}\phi_{ob}+\sum_{n=1}^{\infty}g_{nb}A_{np}\phi_{nb}\right]d\tau' = \frac{\pi}{2F_{ob}}\frac{sen\,p\varphi_o}{p\varphi_o}\left[\theta_i(\tau)-\int_0^\tau p_b(\theta_i,\bar\theta_a,\bar\theta_b,\bar\theta_c)\,d\tau'\right] \tag{B4}$$

for $p=1,2,...,N$,

where $A_{np}=A_{pn}=\frac{1}{\varphi_o}\int_0^{\varphi_0}cosn\,\varphi\cos p\varphi\,d\varphi$ and

$\Lambda_b=2B_{ib}F_{ob}\varphi_o/\pi=h_be_b\Delta t_c/\rho_bc_b\pi r_b^2$.

By replacing θ_c given by equation (23) in equation (26), and performing the integrals in the angle φ it leads to

$$\frac{\phi_{oc}(\tau)}{\Lambda_c}+\left[\int_0^{\tau}\frac{(\phi_{oc}(\tau')-\gamma\phi_{oa}(\tau'))}{2}d\tau' + \sum_{n=1}^{\infty}\frac{sen\, n\varphi_o}{n\varphi_o}\int_0^{\tau}e^{-n^2F_{oc}(\tau-\tau')}(\phi_{nc}(\tau')-\gamma\phi_{na}(\tau'))d\tau'\right] \quad \text{(B5)}$$
$$=\frac{\pi}{2F_{oc}}\left[\theta_i-\int_0^{\tau}p_c(\theta_i,\bar{\theta}_a,\bar{\theta}_b,\bar{\theta}_c)d\tau'\right]$$

for $p=0$ and

$$\frac{\phi_{pc}(\tau)}{\Lambda_c}+\left[\frac{sen\, p\varphi_o}{p\varphi_o}\int_0^{\tau}\frac{(\phi_{oc}(\tau')-\gamma\phi_{oa}(\tau'))}{2}d\tau' + \sum_{n=1}^{\infty}A_{np}\int_0^{\tau}e^{-n^2F_{oc}(\tau-\tau')}(\phi_{nc}(\tau')-\gamma\phi_{na}(\tau'))d\tau'\right] \quad \text{(B6)}$$
$$=\frac{\pi}{2F_{oc}}\frac{sen\, p\varphi_o}{p\varphi_o}\left[\theta_i-\int_0^{\tau}p_c(\theta_i,\bar{\theta}_a,\bar{\theta}_b,\bar{\theta}_c)d\tau'\right]$$

for $p=1,2,...,N$

where $\Lambda_c=2B_{ic}F_{oc}\varphi_o/\pi=2h_ce_c\Delta t_c/\rho_cc_c\pi d_c(r_a+r_c)$.
In order to solve the above equations numerically, in terms of the heat fluxes as functions of $\theta_i,\bar{\theta}_a,\bar{\theta}_b$, and $\bar{\theta}_c$, the heat flux unknown functions $\phi_n(\tau)$; n = 1, 2, .. , N are approximated by polygonal functions. For each n, $\phi_n(\tau)$ is expressed by a tent-function as defined below.
For the sub-interval $[\tau_{j-1},\tau_j]$

$$\phi=\phi_j(\tau)=\frac{a_j(\tau-\tau_{j-1})}{\Delta\tau};\ \Delta\tau=\tau_j-\tau_{j-1} \quad \text{(B7)}$$

while for the sub-interval $[\tau_j,\tau_{j+1}]$

$$\phi=\phi_j^+(\tau)=\frac{a_j(\tau+\Delta\tau-\tau)}{\Delta\tau};\ \Delta\tau=\tau_{j+1}-\tau_j \quad \text{(B8)}$$

where a_j is unknown. A polygonal element construction is shown in Figure B.1 where $\phi(\tau_j)=a_j$.

Let us define $\phi_{pa}(\tau_j)=a_{pj}$, $\phi_{pb}(\tau_j)=b_{pj}$, and $\phi_{pc}(\tau_j)=c_{pj}$; $j=1,2,...;\ p=1,2,...N$. Because of the initial conditions, $\phi_{pa}(0)=a_{p1}=0$, $\phi_{pb}(0)=b_{p1}=0$ and $\phi_{pc}(0)=c_{p1}=0$; $p=1,2,...N$. By replacing the heat flux tent-functions in the integral equations, the integrals of the exponential functions in τ at each sub-interval of τ, are rearranged in the following matrix entries,

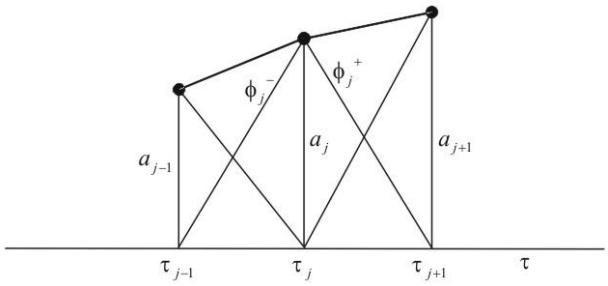

Figure B.1. Composition of tent-functions for polygonal is approximated by discretization

$$B_{kj}^{\pm}=\sum_{m=1}^{\infty}A_{jk}^{\pm}(\alpha_m) \quad \text{(B9)}$$

where $A_{jk}^{\pm}$ is evaluated by the following equations

$$A_{kj}^{-}(\beta)=\int_{\tau_{j-1}}^{\tau_j}e^{-\beta(\tau_k-\tau')}\phi_j^-(\tau')d\tau' =\frac{1}{\beta}\left[e^{-\beta(k-j)\Delta\tau}-\left(\frac{e^{-\beta(k-j)\Delta\tau}-e^{-\beta(k-j+1)\Delta\tau}}{\beta\Delta\tau}\right)\right] \quad \text{(B10)}$$

; $j\le k$ and

$$A_{kj}^{+}(\beta)=\int_{\tau_j}^{\tau_{j+1}}e^{-\beta(\tau_k-\tau')}\phi_j^+(\tau')d\tau' =-\frac{1}{\beta}\left[e^{-\beta(k-j)\Delta\tau}+\left(\frac{e^{-\beta(k-j)\Delta\tau}-e^{-\beta(k-j-1)\Delta\tau}}{\beta\Delta\tau}\right)\right] \quad \text{(B11)}$$

; $j\le k-1$, where $\Delta\tau=1/M$ and $\tau_j=j\Delta\tau$; $j=1,2,....,M$, and M is the number time intervals.

$$B_{nkj}^{\pm}=\sum_{m=1}^{\infty}\frac{A_{kj}^{n\pm}(\alpha_m^n)}{(1-n^2/\alpha_m^{n\,2})} \quad \text{(B12)}$$

where α_m and α_m^n are related to the eigen-values of the boundary value problems of heat conduction.

The following matrix equation can be obtained from equations (B1), (B2), (B5) and (B6) [6],

$$\begin{bmatrix}H^{aa} & H^{ac}\\ H^{ca} & H^{cc}\end{bmatrix}\begin{Bmatrix}a\\ c\end{Bmatrix}=\begin{Bmatrix}Q^a\\ Q^c\end{Bmatrix} \quad \text{(B13)}$$

where $a=(a_{ok},a_{1k},a_{2k},...,a_{Nk})$, $c=(c_{ok},c_{1k},c_{2k},...,c_{Nk})$, $Q^a=(Q_{ok}^a,Q_{1k}^a,Q_{2k}^a,...,Q_{Nk}^a)$, $Q^c=(Q_{ok}^c,Q_{1k}^c,Q_{2k}^c,...,Q_{Nk}^c)$, $H_{oo}^{aa}=F_{oc}\gamma\frac{\Delta\tau}{2}+F_{oa}\Delta\tau+2F_{oa}B_{kk}^{a-}$, $H_{on}^{aa}=0$, $H_{po}^{aa}=0$,

$$H^{aa}_{pn} = (F_{oc}\,\gamma\, B^{c-}_{pkk} + 2F_{oa}\, B^{a-}_{pkk})\delta_{pn}, \qquad H^{ac}_{oo} = -F_{oc}\,\frac{\Delta\tau}{2},$$

$$H^{ac}_{on} = 0,\ H^{ac}_{po} = 0,\ H^{ac}_{pn} = -F_{oc}\, B^{c-}_{pkk}\delta_{pn}$$

where $\delta_{pn} = 1$ se $p = n$ e $\delta_{pn} = 0$ se $p \neq n$.

$$H^{ca}_{oo} = -\gamma\,\frac{\Delta\tau}{4},\ H^{cc}_{oo} = \frac{1}{\Lambda_c} + \frac{\Delta\tau}{4},\ H^{ca}_{on} = -\left(\frac{sen\, n\varphi_o}{n\varphi_o}\right)\gamma\, B^{c-}_{nkk},$$

$$H^{ca}_{po} = -\frac{sen\, p\varphi_o}{p\varphi_o}\gamma\,\frac{\Delta\tau}{4}, \qquad H^{ca}_{pn} = -\gamma\, B^{c-}_{nkk}A_{pn},$$

$$H^{cc}_{on} = \left(\frac{sen\, n\varphi_o}{n\varphi_o}\right)B^{c-}_{nkk}, \qquad H^{cc}_{po} = \frac{sen\, p\varphi_o}{p\varphi_o}\,\frac{\Delta\tau}{4},$$

$$H^{cc}_{pn} = \frac{\delta_{pn}}{\Lambda_c} + B^{c-}_{nkk}A_{pn}, \quad ; p,n = 1,2,...,N$$

$$Q^{a}_{ok} = \pi\left[\int_0^{\tau_k}(p_c - p_a)d\tau'\right] - \sum_{j=1}^{k-1}\Big((F_{oc}\,\gamma\,\Delta\tau + 2F_{oa}\,\Delta\tau + 2F_{oa}B^{a-}_{kj} + 2F_{oa}B^{a+}_{kj})a_{oj} - F_{oc}\,\Delta\tau\, c_{oj}\Big) \tag{B14}$$

$$Q^{a}_{pk} = -\sum_{j=1}^{k-1}\Big(F_{oc}\,\gamma(B^{c-}_{pkj} + B^{c+}_{pkj}) + 2F_{oa}(B^{a-}_{pkj} + B^{a+}_{pkj})\Big)a_{pj} + F_{oc}\sum_{j=1}^{k-1}(B^{c-}_{pkj} + B^{c+}_{pkj})c_{pj} \qquad ; p = 1,2,...,N \tag{B15}$$

$$Q^{c}_{ok} = \frac{\pi}{2F_{oc}}\left[\theta_i(\tau_k) - \int_0^{\tau_k} p_c d\tau'\right] - \sum_{j=1}^{k-1}\left[\frac{\Delta\tau}{2}(c_{oj} - \gamma a_{oj}) + \sum_{n=1}^{N}\left(\frac{sen\, n\varphi_o}{n\varphi_o}\right)(B^{c-}_{nkj} + B^{c+}_{nkj})(c_{nj} - \gamma a_{nj})\right] \tag{B16}$$

$$Q^{c}_{pk} = \frac{\pi}{2F_{oc}}\left(\frac{sen\, p\varphi_o}{p\varphi_o}\right)\left[\theta_i(\tau_k) - \int_0^{\tau_k} p_c d\tau'\right] - \sum_{j=1}^{k-1}\left[\left(\frac{sen\, p\varphi_o}{p\varphi_o}\right)\frac{\Delta\tau}{2}(c_{oj} - \gamma a_{oj}) + \sum_{n=1}^{N}A_{np}(B^{c-}_{nkj} + B^{c+}_{nkj})(c_{nj} - \gamma a_{nj})\right] \quad ; p = 1,2,...,N \tag{B17}$$

where $B^{c\pm}_{nkj} = A^{\pm}_{kj}(\beta)$, $\beta = n^2F_{oc}$, $B^{a\pm}_{kj} = \sum_{m=1}^{\infty}A^{\pm}_{kj}(\alpha_m)$, $\alpha_m = \beta^{o\ 2}_m F_{oa}$, $B^{a\pm}_{nkj} = \sum_{m=1}^{\infty}A^{\pm}_{kj}(\alpha^n_m)$, $\alpha^n_m = \beta^{n\ 2}_m F_{oa}$.

The following matrix equation can be obtained from equations (B3) and (B4),

$$\left[H^b\right]\left\{b\right\} = \left\{Q^b\right\} \tag{B18}$$

where

$b = (b_{ok}, b_{1k}, b_{2k}, ..., b_{Nk})$, $Q^b = (Q^b_{ok}, Q^b_{1k}, Q^b_{2k}, ..., Q^b_{Nk})$,

$$H^b_{oo} = \frac{1}{\Lambda_b} + \frac{\Delta\tau}{2} + B^{b-}_{kk}, \qquad H^b_{on} = 2\frac{sen\, n\varphi_o}{n\varphi_o}B^{b-}_{nkk},$$

$$H^b_{po} = \frac{sen\, p\varphi_o}{p\varphi_o}\left(\frac{\Delta\tau}{2} + B^{b-}_{kk}\right), \quad H^b_{pn} = \frac{\delta_{pn}}{\Lambda_b} + 2A_{pn}B^{b-}_{nkk},$$

$$Q^{b}_{ok} = \frac{\pi}{2F_{ob}}\left[\theta_i(\tau_k) - \int_0^{\tau_k} p_b d\tau'\right] - \sum_{j=1}^{k-1}\left[(\Delta\tau + B^{b-}_{kj} + B^{b+}_{kj})b_{oj} + 2\sum_{n=1}^{N}\frac{sen\, n\varphi_o}{n\varphi_o}(B^{b-}_{nkj} + B^{b+}_{nkj})b_{nj}\right] \tag{B19}$$

$$Q^{b}_{pk} = \frac{\pi}{2F_{ob}}\frac{sen\, p\varphi_o}{p\varphi_o}\left[\theta_i(\tau_k) - \frac{\pi}{2F_{ob}}\int_0^{\tau_k} p_b d\tau'\right] - \sum_{j=1}^{k-1}\left[\frac{sen\, p\varphi_o}{p\varphi_o}(\Delta\tau + B^{b-}_{kj} + B^{b+}_{kj})b_{oj} + 2\sum_{n=1}^{N}A_{np}(B^{b-}_{nkj} + B^{b+}_{nkj})b_{nj}\right] \quad ; p = 1,2,...,N \tag{B20}$$

where $B^{b\pm}_{kj} = \sum_{m=1}^{\infty}A^{\pm}_{kj}(\alpha_m)$, $\alpha_m = \beta^{o\ 2}_m F_{ob}$, $B^{b\pm}_{nkj} = \sum_{m=1}^{\infty}A^{\pm}_{kj}(\alpha^n_m)$, $\alpha^n_m = \beta^{n\ 2}_m F_{ob}$.

The ordinary non-linear differential equations (1), (6), (9), and (16) of the text are solved by the Runge-Kutta method, together with the matrix equations (B13) and (B18), iteratively and recursively in the variable τ. The detailed description of the numerical scheme is also reported in [6]. For the limiting-case respective to $\varphi_o = 0$, $\frac{sen\, p\varphi_o}{p\varphi_o}$ and A_{pq} appearing in the above matrix entries are proved to be equal to the unity for any p, q = 1,2,…, N. For this special case, it is assumed that the limit of the parameter Λ_b for φ_o tending to zero is regular and physically meaningful.

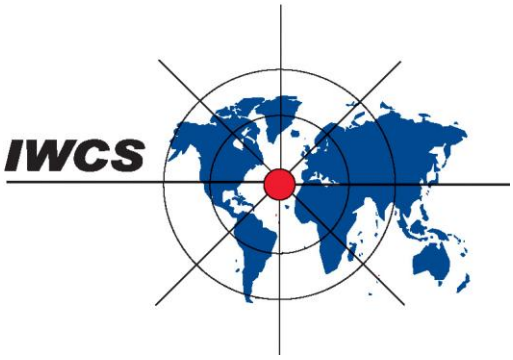

International Wire & Cable Symposium (IWCS) Inc.

174 Main Street,
Eatontown,
New Jersey 07724
USA

Telephone - +1-732-389-0990; Fax - +1-732-389-0991

www.iwcs.org

Editor: Dr Alistair Duffy
De Montfort University, Leicester UK